INTERNATIONAL JOURNAL OF
NUMERICAL ANALYSIS AND MODELING
Volume 9, Number 3, Pages 667–683

A HYBRID UPSCALING PROCEDURE FOR MODELING OF FLUID FLOW IN FRACTURED SUBSURFACE FORMATIONS

BIN GONG AND GUAN QIN

This paper is dedicated to the memory of Dr. Magne S. Espedal

Abstract. Natural fractures reside in various subsurface formations and are at various length scales with different intensities. Fluid flow in fractures, in matrix and between matrix and fractures are following different flow physics. It is thus a great challenge for efficiently modeling and simulation of fluid flow in fractured media due to the multi-scale and multi-physics nature of the flow processes.

Traditional dual-porosity and dual-permeability approach represents fractures and matrix as different continuum. The transfer functions or shape factors are derived to couple the fluid flow in matrix and fractures. The dual-porosity and dual-permeability model can be viewed as a multi-scale method and the transfer functions are used to propagate fine-scale information to the coarse-scale reservoir simulation. In this paper, we perform a detailed study to better understand the optimal way to propagate the fracture information to the coarse-scale model based on the detailed fracture characterization at fine-scale.

The Discrete Fracture Modeling (DFM) approach is used to represent each fracture individually and explicitly. The multiple sub-region (MSR) method is previously used for upscaling calculations based on fine-scale flow solution by finite volume method on the DFM. The MSR method is the most appropriate upscaling procedure for connected fracture network but not for disconnected fractures. In this paper, we propose an adaptive hybrid multi-scale approach that combines MSR and DFM adaptively for upscaling calculation for complex fractured subsurface formations that usually involve both connected fracture network and disconnected fractures. The numerical results suggest that adaptive hybrid multi-scale approach can provide accurate upscaling results for flow in a complicated geological system.

Key words. fractures, porous media flow, multi-scale, upscaling

1. Introduction

Natural fractures reside in various subsurface formations and are at various length scales with different intensities. The accurate modeling of flow through such systems is important for many types of problems, including the management of energy resources (oil, gas, geothermal) and geologically sequestered CO_2, as the fractures often provide the primary conduits for flow.

Fluid flow in fractures, in matrix and between matrix and fractures are following different flow physics. Moreover, fracture distribution in subsurface formation usually displays significant variation in connectivity and size over the formation. Large and strongly connected fractures are typically located near bedding planes and fault zones, while small and disconnected fractures are usually located away from those regions. In addition, as discussed in [16], the dimensions and spatial frequency of fractures are impacted by the thickness of the confining stratigraphy. The variation in fracture properties, especially fracture connectivity, requires to model different fracture zones using different numerical treatments to achieve accurate upscaling results as discussed in [4, 14, 18].

Received by the editors March 2, 2011 and, in revised form, August 29, 2011.
2000 *Mathematics Subject Classification.* 35R35, 49J40, 60G40.

The dual-porosity and dual-permeability model starts from the assumption that fractured porous media can be considered as the overlapping of a matrix continuum and a fracture continuum, which are locally connected to each other. The basic assumption in the dual-porosity and dual-permeability approach is that the global flow occurs only through the fractures and the matrix is only locally connected to the fracture networks and serves as the storage space for fluids [19]. The dual-porosity and dual-permeability model can be viewed as a multi-scale method, in which flow between matrix and fractures occurs on the fine-scale and flow through fractures on the coarse-scale. Since fracture permeability is extremely higher in comparison with matrix permeability, an additional assumption in [19] is that the fine-scale flow in matrix blocks reaches pseudo-steady state instantly after the global flow starts, at which the time rate of change of pressure is a constant [19]. The transfer functions or shape factors can thus be derived to couple the fluid flow in matrix and fractures based on the fracture characterization and are used to propagate the fine-scale information to the coarse-scale reservoir simulation. The analytical form of the transfer functions can be derived based on approximated fracture model [1, 2, 13, 15, 19, 20, 21]. Numerical upscaling procedure needs to be applied to accurately compute transfer functions based on realistic fracture characterization.

In previous work, we have performed global flow simulations using discrete fracture modeling (DFM) for fine-scale reference solutions and multiple subregion method (MSR) for upscaling treatment [6, 7]. DFM represents each fracture individually and explicitly, which requires unstructured gridding of fracture-matrix system using 3D (Delaunay) triangulations and transmissibility evaluation between each pair of adjacent elements [11]. MSR is a generalized dual-porosity and dual-permeability approach that numerically calculates the mass transfer between fractures and matrix based on discrete fracture information and multiple subregions are used to characterize the global flow regime at pseudo-steady state [6, 12].

The assumption of instant pseduo-steady state is not valid if the transient period is too long, which can happen if the formation contains disconnected or locally connected fracture network, or if the coarse blocks contain wells. Therefore, the MSR is an appropriate upscaling procedure when all of the fractures are globally connected so matrix and fractures exchange fluid locally while large-scale flow only occurs through the fracture network [12]. The global use of MSR loses accuracy if reservoir contains large portion of disconnected fractures, or the disconnected fractures are in key regions such as near-wells. In this paper, we present some preliminary numerical results using an adaptive hybrid multi-scale approach, which combines MSR and DFM based on fracture characterization. The numerical results suggest that adaptive hybrid multi-scale approach can provide accurate upscaling results for flow in a complicated geological system.

This paper proceeds as follows. First, we briefly review dual-porosity model and, the DFM and the MSR method for upscaling procedure. Second, the hybrid methodology is described and the computations for the internal and inter-block connections are explained for the multi-scale approach that integrates DFM and MSR. Next the hybrid approach is applied to several cases (2D and 3D) for two-phase, three-phase and compositional flow examples. These results demonstrate the improvement in accuracy attainable from the hybrid procedure. We also discuss computational demands for this approach, which are important to consider because the hybrid method is more expensive than the global MSR procedure.

2. Dual-porosity model

The dual porosity model assumes that fractured porous media can be considered as the overlapping of a matrix continuum that is porous medium with well-defined porosity and permeability and a fracture continuum, in which they are locally connected to each other. The governing equations can be written for each continuum by combining the mass conservation and Darcy's law:

$$\phi_m \frac{\partial \rho_m}{\partial t} - \nabla \cdot (\frac{k_m \rho_m}{\mu} \nabla p_m) = -\tau, \tag{1}$$

$$\phi_f \frac{\partial \rho_f}{\partial t} - \nabla \cdot (\frac{k_f \rho_f}{\mu} \nabla p_f) = q + \tau, \tag{2}$$

where the subscript m and f stand for matrix and fracture, respectively, and k is the permeability of the subsurface formation. p denotes fluid pressure, ρ and μ are fluid density and viscosity, respectively.

In the equation (1) and (2), τ is the flux exchange between matrix and fracture, q is the source/sink term. Notice that q only appears in the fracture flow equation, which implies another assumption that the global flow occurs only through the fractures. Matrix is only locally connected to the fracture networks and serves as the storage space for the fluids. Thus, the fracture flow equation should be solved globally on coarse scale and the matrix equation should be solved locally on fine scale. In order to denote this difference, we use γ to represent the coarse scale and use β to represent the fine scale. Equations (1) and (2) can then be written in a format similar to asymptotic analysis:

$$\phi_m \frac{\partial \rho_m}{\partial t} - \nabla_\beta \cdot (\frac{k_m \rho_m}{\mu} \nabla_\beta p_m) = 0, \quad \text{(matrix)} \tag{3}$$

$$\phi_f \frac{\partial \rho_f}{\partial t} - \nabla_\gamma \cdot (\frac{k_f \rho_f}{\mu} \nabla_\gamma p_f) = q + \tau. \quad \text{(fracture)} \tag{4}$$

Since the matrix flow equation is written locally on fine scale, the flux exchange term τ is defined as the average over matrix blocks on coarse grid:

$$\tau = -\frac{1}{V_m} \int_{V_m} \phi_m \frac{\partial \rho_m}{\partial t} dv = \frac{1}{V_m} \int_{V_m} \nabla_\beta \cdot (\frac{k_m \rho_m}{\mu} \nabla_\beta p_m) dv. \tag{5}$$

Consequently, the key issue in dual-porosity model is the accurate approximation of τ, which involves upscaling treatment and [1, 5] provide detailed discussion on the numerical solution techniques.

Originally, Warren and Root [19] assume that the fine-scale flow in matrix blocks reaches pseudo-steady state in which the pressure in the entire system changes with a constant rate, i.e. $\frac{\partial p}{\partial t} = const$ instantly after the global flow starts. Thus, the pressure in matrix blocks can be approximated by an average pressure $\bar{p}_m$ and

$$\tau = \alpha \frac{k_m}{\mu} (p_f - \bar{p}_m). \tag{6}$$

In Equation (6), α stands for the transfer function or shape factor. By assuming regularly spaced fractures, α can be calculated analytically [13, 15, 19, 20, 21].

The assumption of instant pseudo-steady state is not valid if the coarse grid block is big or the matrix permeability is small, which usually is the case in field-scale reservoir simulations. Furthermore, complex fracture distribution in real world makes even harder to compute transfer function analytically. Numerical upscaling procedure presents the advantages in computing τ.

3. Discrete Fracture Modeling and Multiple Sub-region Method for Upcaling

3.1. Discrete Fracture Modeling (DFM). Discrete fracture modeling represents each fracture as a geometrically well-defined entity using highly resolved unstructured grids as illustrated in Figure 1. In the DFM, fractures are a collection of 1D elements that are the edges of matrix elements in 2D cases. Similar methodology is extended for 3D DFM. Since its first introduction in the late 1970s, many

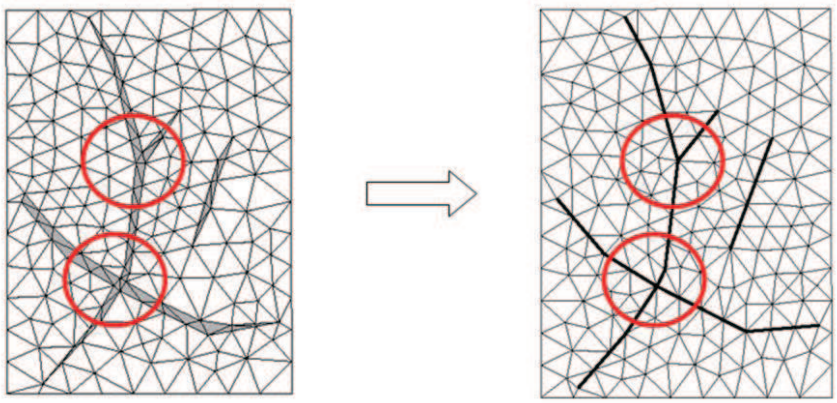

FIGURE 1. Detailed discrete fracture realization to discrete fracture modeling (DFM) [11]

researchers have developed numerical algorithms for solving flow problems based on DFM such as [3, 8, 10, 17]. Karimi-Fard et al.(2004) presented a finite-volume algorithm for solving flow problem on DFM and applied a connection list to represent the unstructured grid. This method is applicable for 2D and 3D systems with multiphase flow and we use this algorithm for solving flow problems in this paper [11].

DFM reduces the overall number of elements and significantly simplifies griding procedure, especially in 3D systems. However, the use of DFM for flow modeling at the field scale is still too computationally demanding. An appropriate upscaling strategy needs to be considered for an efficient field-scale simulation.

3.2. Multiple Sub-region Method (MSR) for Upscaling Calculation. Karimi-Fard (2006) and Gong (2008) introduced a systematic upscaling methodology that constructs a generalized dual-porosity/dual-permeability model from fine-scale discrete fracture characterizations [6, 12]. This technique, referred to as a multiple subregion (MSR) method, introduces local subregions (or subgrids) to resolve dynamics within the matrix and provides appropriate coarse-scale parameters that describe fracture-fracture, matrix-fracture and matrix-matrix flow. The construction of multiple subregions can be viewed as a generalized dual-porosity/dual-permeability approach when the number of subregions inside each coarse block is reduced to 2 - one for the fracture and the other for the matrix. In traditional dual-porosity and dual-permeability approach, the flux exchange τ in (1) and (2) is computed by (6), where the shape factor or transfer function α is approximated by assuming regular fracture distribution within coarse blocks. In comparison, MSR is advantageous in representing a realistic fracture characterization while upscaling the flux exchange between matrix and fractures since the construction of subregions involves local

pressure solve based on the actual fracture distribution. Besides, with more than 2 subregions in each coarse block, MSR is capable of modeling transient effects inside the matrix thus provides a higher degree of accuracy.

The MSR method basically involves two steps. In the first step, a single phase and single porosity flow problem is solved inside each coarse cell with no-flow boundary condition and a well with constant injection flow rate inside the fracture network. The overall pressure of each coarse cell will increase with time and reach a pseudo-steady state profile after a transient period [6, 12]. Due to the high permeability of the fracture network, the pressure inside the fractures is approximately the same and the pressure variation inside the matrix behaves like a diffusion process. The shapes of the iso-pressure curves at pseudo-steady state depend only on the fracture geometry and permeability variation within the coarse cell and are independent of the injection rate and fluid properties. Sub-regions can then be identified based on the pseudo-steady state pressure distribution.

Based on the fine-scale pressure solution, each coarse block can be subdivided into non-overlapping sub-regions,

$$\Omega^k = \bigcup_{i=1}^{n} \Omega_i^k, \tag{7}$$

where Ω_i^k stands for the ith sub-region in Ω^k. This subdivision is performed by sorting all of the fine-scale cells in coarse cell k according to their pressure values from the maximum pressure, p_{max}^k, to the minimum pressure, p_{min}^k. The first subregion Ω_1^k is constructed from the fine-scale fracture network. As the solution is obtained by injecting fluid inside the fracture network, the sub-region Ω_1^k has the highest average pressure. The remaining matrix cells are then grouped into $(n-1)$ groups defining $(n-1)$ additional subregions. The iso-pressures that define the borders of each subregion are obtained by minimizing the summation of pressure variance inside each subregion [6, 12].

The bulk volume V_i^k of each sub-region and the average porosity can be computed once Ω_i^k are determined. The average pressure $\bar{p}_i^k$ and density $\bar{\rho}_i^k$ can be computed using pore-volume weighted average. The transmissibility of the sub-region can be calculated by the mass accumulation within each sub-region at pseudo-steady state. This quantity, designated A, is computed via:

$$A_i^k = \sum_{j \in \Omega_i^k} v_j \phi_j \frac{\partial \rho_j}{\partial t} \tag{8}$$

v_j is the volume for fine cell j, $j \in \Omega_i^k$ means that for all fine cells in subregion Ω_i^k.

At pseudo-steady state, $\frac{\partial \rho_j}{\partial t}$ is constant and the accumulation term is proportional to the pore volume of the subregion. The flow rate between two subregions $n-1$ and n is equal to the mass accumulation in subregion n:

$$Q_{n-1,n}^k = A_n^k. \tag{9}$$

The other inter-subregion flow rates are computed using:

$$Q_{i,i+1}^k = A_{i+1}^k - Q_{i+1,i+2}^k, \quad i = 1, 2, \cdots, n-2, \tag{10}$$

which simply states that the net mass flow into (or out of) sub-region Ω_i^k is balanced by the accumulation term.

From the local solution we have the sub-region pressures ($\bar{p}_i^k$ and $\bar{p}_{i+1}^k$) and the flow rates between them ($Q_{i,i+1}^k$). We can thus compute the transmissibility

between adjacent sub-regions using the following equation [6, 12]:

$$T^k_{i,i=1} = \frac{Q^k_{i,i+1}\mu}{\bar{\rho}^k_i(\bar{p}^k_i - \bar{p}^k_{i+1})}, \quad i = 1, 2, \cdots, n-2. \tag{11}$$

These transmissibilities combined with the associated sub-region volumes, V^k_i, and porosities, $\bar{\phi}^k_i$, fully define the local matrix-fracture and matrix-matrix flow model inside each coarse cell along with the connection list that define the linkages among the sub-regions [6, 12].

The second step in MSR procedure is to compute the transmissibility between the two adjacent coarse cells Ω^k and Ω^l based on the fine-scale information. A steady-state flow problem is solved with a pressure difference imposed between the two boundaries. The average pressure and fluid properties inside each block, as well as the flow rate $Q^{k,l}$ through the interface between the blocks, are computed from the local fine-scale solution. The transmissibility can then be determined via [6, 12]:

$$T^{k,l} = \frac{Q^{k,l}\mu}{\rho(\bar{p}^k - \bar{p}^l)}. \tag{12}$$

The mass flow rate $Q^{k,l}$ is computed over the entire interface, though it will be dominated by flow through the fractures when the fracture network is connected (as it generally will be for models in which a dual-porosity formulation is applicable). For those blocks in which the fractures are disconnected, this treatment will provide a reasonable approximation for $T^{k,l}$ even in cases when the inter-block flow is from the matrix in block k to the matrix in block l [12].

The geometry of the local subregions, as well as the required parameters for the coarse-scale model, are determined efficiently from local single-phase flow solutions using the underlying discrete fracture model. The subregions thus account for the fracture distribution and can represent accurately the matrix-matrix and matrix-fracture transfer.

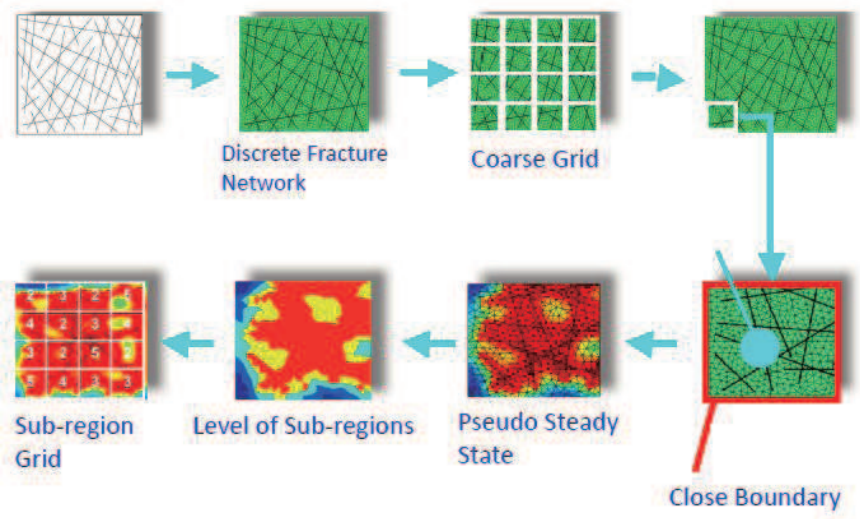

FIGURE 2. The procedure of multiple sub-region method [7].

Figure 2 is the outline of the first step of MSR upscaling procedure, in which the fine-scale DFM is represented by a 4×4 Cartesian grid on coarse level. The bottom left image illustrates the coarse grid with different level of sub-regions inside each coarse block after the MSR procedure and the subregion grid is represented by cell groups in different colors inside each coarse block. The geometry of the local subregions, as well as the required parameters for the coarse-scale model, are determined efficiently from local single-phase flow solutions using the underlying discrete fracture model. The subregions thus account for the fracture distribution and can represent accurately the matrix-matrix and matrix-fracture transfer.

4. Methodology for Hybrid DFM/MSR Procedure

The proposed hybrid method models the coarse blocks that contains disconnected fractures based on the DFM representation and others using the MSR approach for upscaling calculations. The subregion geometry, internal transmissibilities between subregions for MSR coarse cells and transmissibilities between MSR coarse cells are determined by MSR upscaling procedure as previously described in [6, 12]. The internal connections for DFM blocks or groups of blocks remain in the fine-scale form. The transmissibilities are determined directly from the discretization on the underlying unstructured fine-scale grid. The key issue in the hybrid approach is thus the evaluation of the transmissibility between the adjacent blocks that are modeled by DFM and MSR, respectively.

Figure 3 illustrates two adjacent coarse blocks in which the left block contains connected fractures and the right one contains disconnected fractures. MSR is applied for upscaling calculations on the left block and DFM for the fine-scale flow simulation on the right block as illustrated in Figure 4. We will use Figure 3 to explain the procedure to evaluate the transmissibilities between those two adjacent blocks that are modeled by MSR and DFM, respectively. The proposed procedure can be applied in both 2D and 3D scenarios.

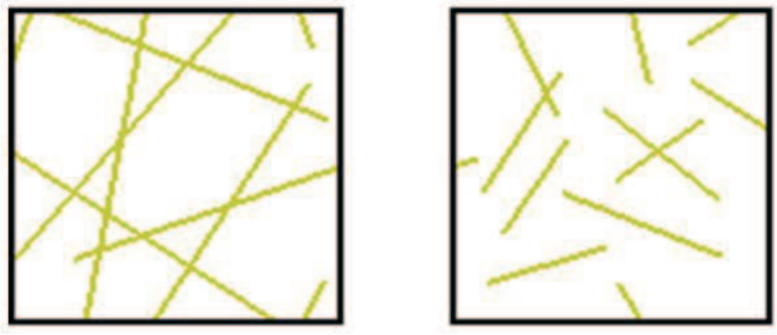

FIGURE 3. Motivation for hybrid method: coarse blocks to be modeled using MSR (left) and DFM (right)

In Figure 4, the MSR block on the left contains four matrix subregions that are labeled by different colors and, the DFM block on the right, by contrast, is fully unstructured and contains 707 triangular cells.

Figure 5 illustrates the linkage between the MSR block k and the DFM block l in Figure 4, in which each subregion on MSR block is connected to all the corresponding fine-scale elements on DFM block through a physical interface with which they

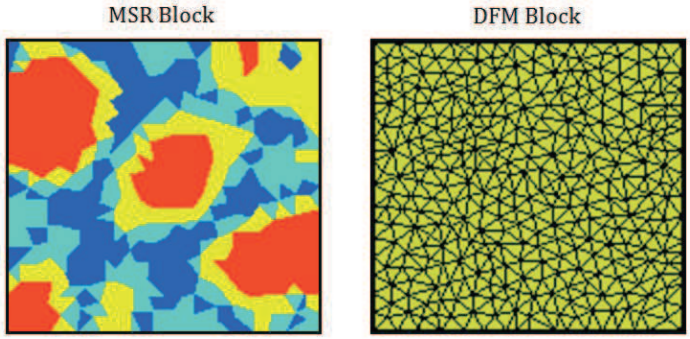

FIGURE 4. Illustration of matrix subregions for MSR block (left) and fine cells for DFM block (right)

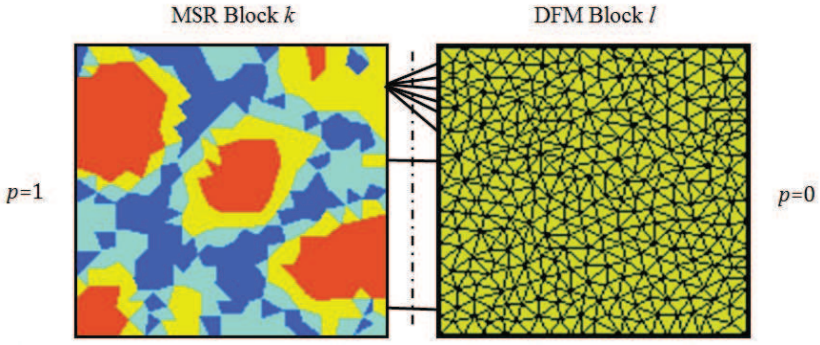

FIGURE 5. Inter-block connection determination for neighboring MSR and DFM blocks

share. As illustrated in Figure 5, the 4th subregion in yellow color from the MSR block is connected to all of the fine cells in the DFM block with which it shares a physical interface. Connections between other subregions in block k and fine cells in block l are defined in a similar fashion.

The hybrid model thus involves connections between particular subregions in MSR blocks and multiple fine cells in DFM blocks. To compute the actual transmissibility values, a steady-state single-phase flow problem is solved with a pressure difference imposed between the two boundaries as illustrated in Figure 5. This solution is performed on the underlying discrete fracture representation. We designate the superscript $k(i)$ to denote subregion i in the MSR block k and $l(j)$ to denote fine cell j in DFM block l. The average pressure and fluid properties inside each subregion, as well as the flow rate $Q^{k(i),l(j)}$ through the interface between the blocks, are computed from the local fine-grid solution. The transmissibility can then be determined via:

$$T^{k(i),l(j)} = \frac{Q^{k(i),l(j)}\mu}{\rho(\bar{p}^{k(i)} - \bar{p}^{l(j)})}, \tag{13}$$

where all quantities are as previously defined. The mass flow rate $Q^{k(i),l(j)}$ is computed over the shared interface of sub-region i in the MSR block k and fine cell j in the DFM block l. We then apply equation (13) for the determination of each of the required transmissibilities.

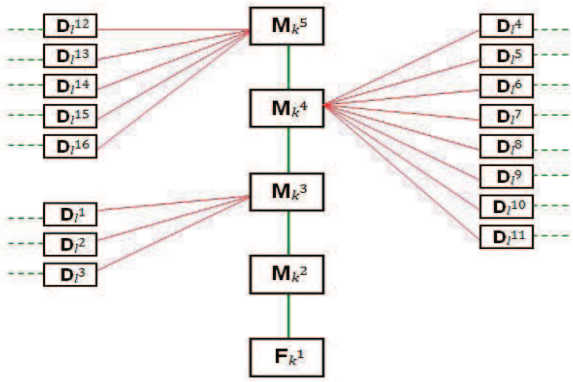

FIGURE 6. Sketch of connection list between one MSR block and one DFM block (setting corresponds to Figure 5)

The connection list is more complicated in this case than it is for the MSR procedures described in our previous work [6, 9, 12]. A portion of the connection list for the case considered above is shown in Figure 6, where the MSR block k is connected to DFM block l. The MSR block k is divided into one fracture subregion F_k^1 and four matrix subregions M_k^1, M_k^2, M_k^3, and M_k^4. The DFM block l consists of 16 fine cells denoted as D_l^1, D_l^2,...D_l^{16}. Green and red lines represent internal and inter-block connections respectively. This figure illustrates that the 3rd, 4th, and 5th subregions of MSR block k are connected to 3, 8, and 5 fine cells respectively of DFM block l. This connection list is input directly into GPRS for flow simulation. We now present results for several representative cases.

5. Numerical Results

The hybrid method is applied to two 2D cases and a 3D case. In the first example, fractures are connected throughout the reservoir. We model the injection and production well blocks using DFM to better resolve the interactions between the wells and fractures; the other coarse blocks in the model are represented using MSR. In the second case, fractures are disconnected in one portion of the reservoir and we use DFM to model these isolated fractures. In the 3D example, the near-well fractures are disconnected and we use DFM to model them.

Case 1&2: 2D Model with Connected Fractures

As shown in Figure 7, a simple synthetic 2D model containing 32 connected fractures is considered. An injector and producer are located in the lower left and upper right corners of the reservoir, and they both intersect fractures. The coarse blocks that contain wells are labeled in light green color and are the DFM block-s. MSR are employed for upscaling calculations on the other coarse blocks. Two simulations are performed, one for an oil-water system and one for miscible gas injection. For the oil-water flow simulation, we use constant injection rate (500 STB/day) for the injector and constant BHP (4,000 psi) for the producer. For the miscible gas injection simulation, we use the same 6-component fluid characteriza-tion for reservoir oil and injected gas as presented in [9], and apply constant BHP controls for both the injector (12,500 psi) and producer (11,500 psi). Our coarse model is upscaled to 4×4 coarse blocks (MSR blocks contain 5 subregions). This represents a high degree of coarsening and some inaccuracy would be expected in the global MSR model.

Figures 8 and 9 display the simulation results for these cases. We present results for the DFM (reference fine-scale results), global MSR, and hybrid approaches. For both the oil-water (case 1) and miscible gas injection (case 2) simulations, we observe that, although the MSR approach yields a model of reasonable accuracy, the hybrid treatment clearly provides improved accuracy. In fact, the hybrid results are nearly indistinguishable from the reference DFM results.

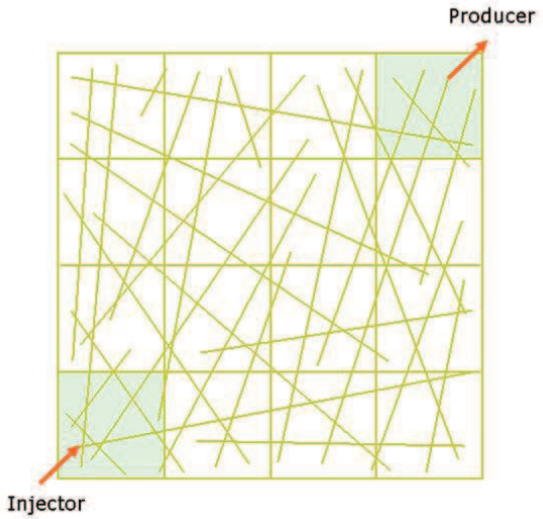

FIGURE 7. Synthetic 2D model with 32 fractures

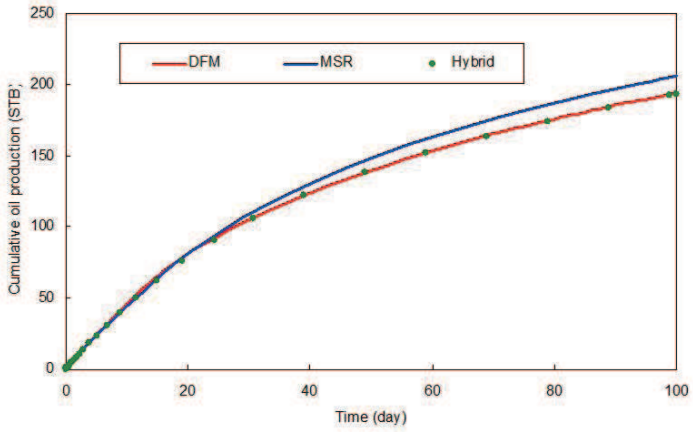

FIGURE 8. Oil recovery results for DFM, global MSR and hybrid solutions for synthetic 2D oil-water flow (case 1)

Case 3: 2D Oil-Water Model with Disconnected Fractures

Figure 10 displays a synthetic model with 35 disconnected fractures in the upper right portion of the model, which are labeled in light green color, and 36 connected fractures elsewhere in the reservoir. This case is somewhat artificial but it would be expected to be a good candidate for the hybrid treatment. We use DFM to model the four blocks in the upper right corner and MSR (with 5 subregions) for the other

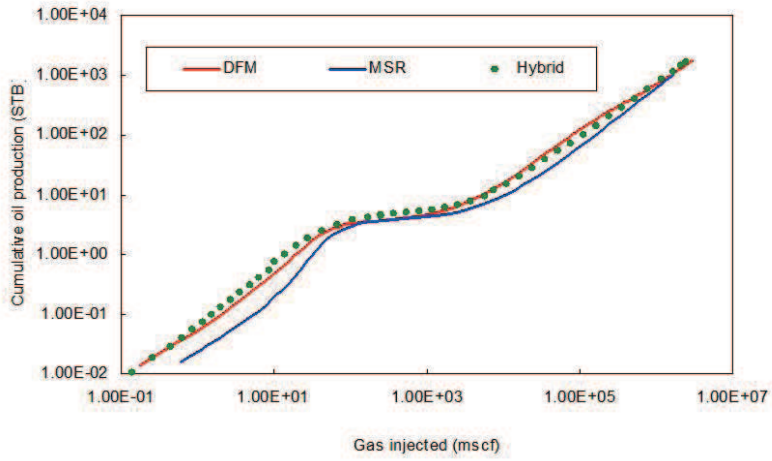

FIGURE 9. Oil recovery results for DFM, global MSR and hybrid solutions for synthetic 2D miscible gas injection (case 2)

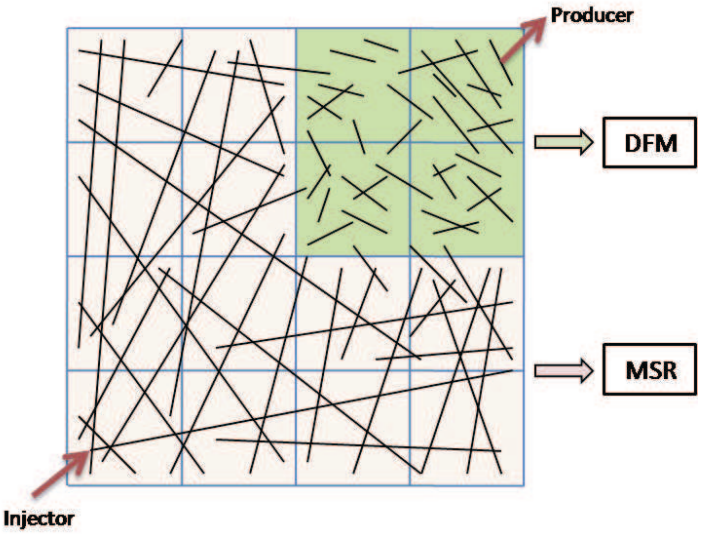

FIGURE 10. Synthetic 2D model with 36 connected fractures and 35 disconnected fractures

twelve blocks. For the wells, we use constant injection rate (500 STB/day)for the injector and BHP control (4,000 psi) for the producer.

Figure 11 displays simulation results for injector BHP. Due to the disconnected fractures in the well region, the MSR solution shows significant error relative to the reference DFM simulation. The hybrid method, by contrast, provides results in close agreement with DFM solution. The hybrid model also gives more accurate results for oil production rate, as shown in Figure 12. This example clearly illustrates the potential for loss of accuracy when the MSR procedure is applied in regions of disconnected fractures and the improved results that can be achieved using the hybrid procedure.

Case 4: 3D Three-Phase Model

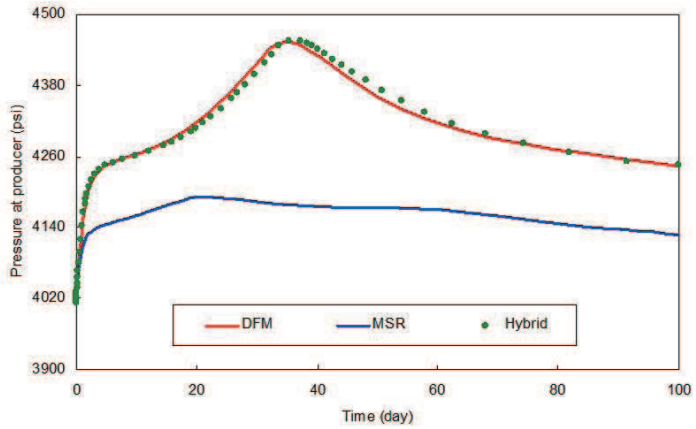

FIGURE 11. Producer BHP results for DFM, global MSR and hybrid solutions for synthetic 2D oil-water flow with disconnected fractures (case 2)

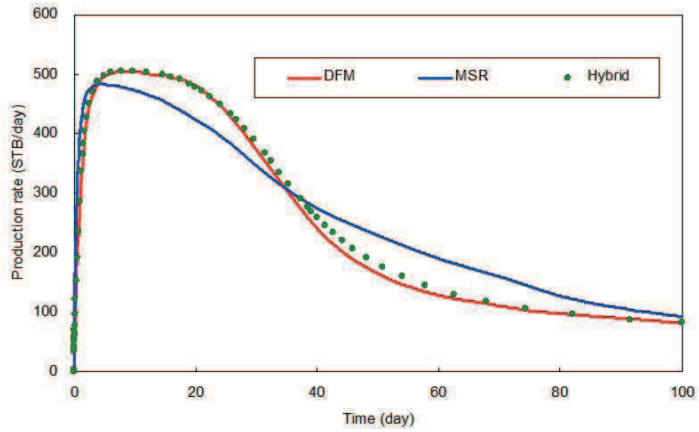

FIGURE 12. Oil production rate results for DFM, global MSR and hybrid solutions for synthetic 2D oil-water flow with disconnected fractures (case 3)

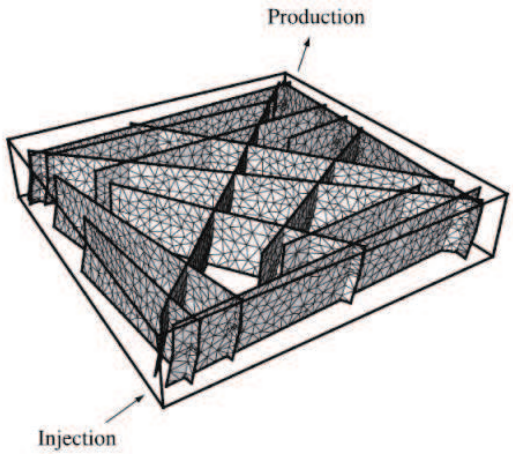

FIGURE 13. Synthetic 3D model with 28 intersecting fractures

The hybrid method is now applied to a 3D three-phase example. Figure 13 represents a $1000 \times 1000 \times 200 ft^3$ model containing 28 intersecting fractures. The fractures are near-vertical though they do have slight inclination. This model is discretized using 52,059 cells (5,247 triangles are for the fractures and 46,812 tetrahedra for the matrix). This simulation domain and fracture configuration is the same as in the 3D case in [12]. The initial reservoir pressure is 4,783 psi and the system is initially saturated with oil and connate water ($S_{wi} = S_{wc} = 0.12$). Water is injected at constant rate (1,000 bbl/day) at one edge and fluid is produced from the opposite edge using a constant BHP (3,500 psi) control as shown in Figure 13. The bubble point for reservoir fluid is 4,014.7 psi. For this case, the MSR demonstrated reasonable accuracy compared to DFM when the upscaled model has a coarse grid of $9 \times 9 \times 3$ in [12]. We now apply a $4 \times 4 \times 1$ coarse grid for MSR upscaling. This coarser MSR model is expected to yield less accurate simulation results. We then apply the hybrid approach to model the injection and/or production well blocks using DFM. The other coarse blocks are treated using MSR with 5 subregions.

Figures 14-16 display the simulation results (gas and oil production rates and pressure at the injector) for the 3D three-phase case. Again, we present results for the DFM, global MSR, and hybrid approaches. We observe that the MSR approach using the $4 \times 4 \times 1$ coarse grid shows substantial error, especially at early time. By resolving the injection and production coarse blocks explicitly using DFM ("Hybrid 1"), the hybrid treatment clearly provides significantly improved accuracy. Improvement over MSR is also observed when we only treat the injection block in DFM ("Hybrid 2") or production block in DFM ("Hybrid 3"). This set of cases demonstrated the advantage of the hybrid models in resolving the near-well regions in finer scale to better represent the actual flow.

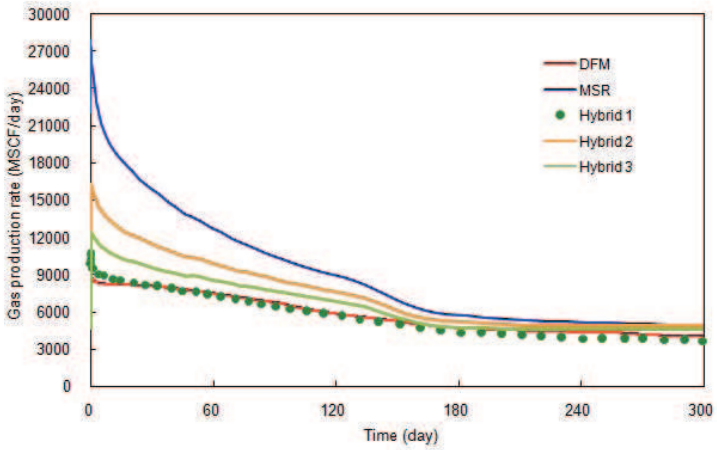

FIGURE 14. Gas production rate results for DFM, global MSR and hybrid solutions for synthetic 3D three-phase flow (case 4)

6. Discussions

The results shown in the application section demonstrate the improved accuracy of the hybrid approach. This improvement results from the use of finer resolution in some regions of the model and therefore leads to increased computational cost, which we now quantify. Compared to the MSR approach, the increased numerical

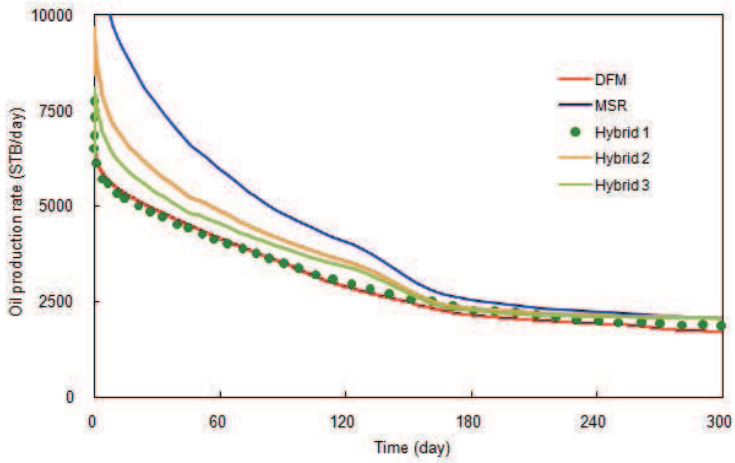

FIGURE 15. Oil production rate results for DFM, global MSR and hybrid solutions for synthetic 3D three-phase flow (case 4)

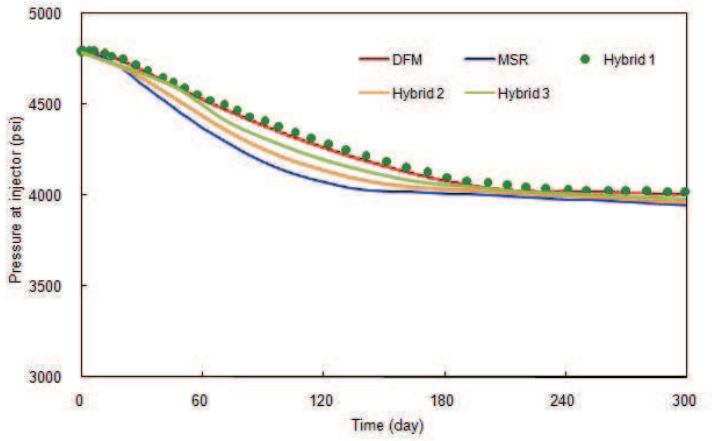

FIGURE 16. Producer BHP results for DFM, global MSR and hybrid solutions for synthetic 3D three-phase flow (case 4)

burden will depend on the number of DFM coarse blocks. Tables 1-4 below summarize the problem size and simulation time for the DFM, global MSR and hybrid approaches for the four cases studied in this paper. All simulations were performed on a 2.66 GHz, Intel CoreDuo CPU.

TABLE 1. Comparison of problem size and simulation time for DFM, global MSR, and hybrid approaches for case 1

	Number of Cells	Number of Connections	Simulation Time (s)
DFM	4659	7619	92
MSR	80	88	2.2
Hybrid	647	1203	14

It is clear from Tables 1-4 that the hybrid treatment leads to many more cells and connections. For these examples, the global MSR offers about a two-order

TABLE 2. Comparison of problem size and simulation time for DFM, global MSR, and hybrid approaches for case 2

	Number of Cells	Number of Connections	Simulation Time (s)
DFM	4659	7619	245
MSR	80	88	3.6
Hybrid	647	1203	35

TABLE 3. Comparison of problem size and simulation time for DFM, global MSR, and hybrid approaches for case 3

	Number of Cells	Number of Connections	Simulation Time (s)
DFM	11677	18460	605
MSR	80	88	8
Hybrid	2909	4610	56

TABLE 4. Comparison of problem size and simulation time for DFM, global MSR, and hybrid approaches for case 4

	Number of Cells	Number of Connections	Simulation Time (hr)
DFM	52,059	103,944	19.8
MSR	80	88	0.2
Hybrid 1	8,019	16,568	2.6
Hybrid 2	3,552	6,991	0.5
Hybrid 3	3,817	7,565	0.6

of magnitude speed up relative to the reference DFM, while the hybrid procedure provides only about a one-order of magnitude speed up relative to DFM. The computational requirements for the hybrid method will directly depend on the number of fine cells included. The timings in Tables 1-4 suggest that it will be important to limit the number of regions that are fully resolved, or to model these regions using a coarse DFM.

7. Concluding Remarks

In this paper, we have proposed an adaptive multi-scale hybrid upscaling procedure. We presented preliminary numerical results by the hybrid procedure that represents some reservoir zones using the MSR for upscaling calculations and other zones using the DFM approach. The hybrid upscaling procedure generalizes the MSR representation, which may encounter problems when applied to reservoir regions with disconnected fractures. In addition, the hybrid approach enables enhanced accuracy in key reservoir zones such as the near-well region. The examples clearly demonstrate the improved accuracy of the hybrid approach, though the additional computational costs (relative to global MSR) of using this method are significant.

It will therefore be important to develop procedures for determining appropriate treatments for reservoir zones in large models. This determination, which was not considered here, might involve first computing various fracture statistics (such as length and connectivity measures). These could then be used to prescribe the appropriate modeling technique for the various reservoir zones. It may also be possible to incorporate some type of iteration procedure in order to assure self-consistency in the model. In analogy to local-global upscaling procedures in [4], this could entail performing a global solution for a simplified problem with the

initial hybrid model and then using this simulation result to determine the proper treatment for each reservoir zone.

Acknowledgments

The second author would like to thank the Center for Fundamentals of Subsurface Flow at School of Energy Resources, University of Wyoming. Both authors would like to thank Sinopec Corporation for their generous support in this research. SUPRI-B research group of Stanford University provides General Purpose Research Simulator (GPRS) for the numerical simulation study in this research.

References

[1] T. Arbogast. Gravitational forces in dual-porosity systems: I. Model derivation by homogenization. *Transport in Porous Media*, 13(2):179–203, 1993.

[2] T. Arbogast, J. Douglas Jr, and U. Hornung. Derivation of the double porosity model of single phase flow via homogenization theory. *Siam J. Math. Anal*, 21(4):823–836, 1990.

[3] R. Baca, R. Arnett, and D. Langford. Modelling fluid flow in fractured-porous rock masses by finite-element techniques. *International Journal for Numerical Methods in Fluids*, 4(4):337–348, 1984.

[4] I. Bogdanov, V. Mourzenko, J. Thovert, and P. Adler. Effective permeability of fractured porous media in steady state flow. *Water Resources Research*, 39(1):1023, 2003.

[5] J. Douglas Jr. and T. Arbogast. Dual porosity models for flow in naturally fractured reservoirs. In *Dynamics of fluids in hierarchical porous media. Academic press, London.*, 1990.

[6] B. Gong, M. Karimi-Fard, and L. Durlofsky. Upscaling discrete fracture characterizations to dual-porosity, dual-permeability models for efficient simulation of flow with strong gravitational effects. *SPE Journal*, 13(1):58–67, 2008.

[7] B. Gong, G. Qin, C. Douglas, and S. Yuan. Detailed Modeling of the Complex Fracture Network and Near-well Effects of Shale Gas Reservoirs. In *SPE Middle East Unconventional Gas Conference and Exhibition*, 2011.

[8] H. Hægland, A. Assteerawatt, H. Dahle, G. Eigestad, and R. Helmig. Comparison of cell- and vertex centered discretization methods for flow in a two-dimensional discrete fracture-matrix system. *Adv. Water Resour.*, 32(12):0309–1708, 2009.

[9] M. Hui, J. Kamath, W. Narr, B. Gong, and R. Fitzmorris. Realistic modeling of fracture networks in a giant carbonate reservoir. In *International Petroleum Technology Conference*, 2007.

[10] R. Juanes, J. Samper, and J. Molinero. A general and efficient formulation of fractures and boundary conditions in the finite element method. *International Journal for Numerical Methods in Engineering*, 54(12):1751–1774, 2002.

[11] M. Karimi-Fard, L. Durlofsky, and K. Aziz. An Efficient Discrete-Fracture Model Applicable for General-Purpose Reservoir Simulators. SPEJ 9 (2): 227–236. Technical report, SPE-79699-PA, 2004.

[12] M. Karimi-Fard, B. Gong, and L. Durlofsky. Generation of coarse-scale continuum flow models from detailed fracture characterizations. *Water Resources Research*, 42(10):10423, 2006.

[13] H. Kazemi, M. LS, K. Porterfield, and P. Zeman. Numerical simulation of water-oil flow in naturally fractured reservoirs. *Old SPE Journal*, 16(6):317–326, 1976.

[14] S. Lee, M. Lough, and C. Jensen. Hierarchical modeling of flow in naturally fractured formations with multiple length scales. *Water Resources Research*, 37(3):443–455, 2001.

[15] K. Lim and K. Aziz. Matrix-fracture transfer shape factors for dual-porosity simulators. *Journal of Petroleum Science and Engineering*, 13(3-4):169–178, 1995.

[16] J. Long, A. Aydin, S. Brown, H. Einstein, K. Hestir, P. Hsieh, L. Myer, K. Nolte, D. Norton, O. Olsson, et al. Rock Fractures and Fluid Flow, Contemporary Understanding and Applications, 551 pp. *Natl. Acad. Press, Washington, DC*, 1996.

[17] S. Matthäi, A. Mezentsev, and M. Belayneh. Control-volume finite-element two-phase flow experiments with fractured rock represented by unstructured 3D hybrid meshes. SPE93341. In *Proceedings of SPE Reservoir Simulation Symposium, Houston, TX, USA*, 2005.

[18] M. Uba, Y. Chiffoleau, T. Pham, V. Divry, A. Al-Kaabi, and J. Thuwaini. Application of a Hybrid Dual Porosity Dual Permeability Representation of Large Scale Fractures to the Simulation of a Giant Carbonate Reservoir. In *SPE Middle East Oil and Gas Show and Conference*, 2007.

[19] J. Warren and P. Root. The behavior of naturally fractured reservoirs. *Old SPE Journal*, 3(3):245–255, 1963.

[20] Y. Wu and K. Pruess. A multiple-porosity method for simulation of naturally fractured petroleum reservoirs. *SPE Reservoir Engineering*, 3(1):327–336, 1988.

[21] Y. Wu and G. Qin. A generalized numerical approach for modeling mulitphase flow and transport in fractured porous media. *Communications in Computational Physics*, 6:85–108, 2009.

Department of Energy & Resources Engineering, Peking University, Beijing, 100871, China
E-mail: gongbin@coe.pku.edu.cn

Department of Chemical & Petroleum Engineering, University of Wyoming, Laramie, WY 82070, USA
E-mail: gqin@uwyo.edu